

MEASUREMENT OF FRAGMENT PRODUCTION
CROSS SECTIONS IN THE $^{12}\text{C}+^{12}\text{C}$ AND $^{12}\text{C}+^{197}\text{Au}$
REACTIONS AT 62 A MeV FOR HADRONTHERAPY
AND SPACE RADIATION PROTECTION*

S. TROPEA^{a,b}, M. DE NAPOLI^c, C. AGODI^a, A.A. BLANCATO^a
M. BONDI^{a,b}, F. CAPPUZZELLO^{a,b}, D. CARBONE^{a,b}, M. CAVALLARO^a
G.A.P. CIRRONE^a, G. CUTTONE^a, F. GIACOPPO^d, D. NICOLOSI^{a,b}
L. PANDOLA^e, G. RACITI^{a,b†}, E. RAPISARDA^f, F. ROMANO^a
D. SARDINA^a, V. SCUDERI^{a,g}, C. SFIENTI^h

^aINFN — Laboratori Nazionali del Sud, Catania, Italy

^bDipartimento di Fisica e Astronomia, Università degli studi di Catania, Italy

^cINFN — Sezione di Catania, Italy

^dDepartment of Physics, University of Oslo, Norway

^eINFN — Laboratori Nazionali del Gran Sasso, Italy

^fNuclear and Radiation Physics Section

Katholieke Universiteit Leuven, Heverlee, Belgium

^gInstitute of Physics of the ASCR, Prague, Czech Republic

^hJohannes Gutenberg Universität, Institut für Kernphysik
Mainz, Germany

(Received December 2, 2013)

Over the last twenty years, there has been a renewed interest in nuclear fragmentation studies for both hadrontherapy applications and space radiation protection. In both fields, fragmentation cross sections are needed to predict the effects of the ions nuclear interactions within the patient's and the astronaut's body. Indeed, the Monte Carlo codes used in planning tumor treatments and space missions must be tuned and validated by experimental data. However, only a limited set of fragmentation cross sections are available in literature, especially at Fermi energies. Therefore, we have studied the production of secondary fragments in the $^{12}\text{C}+^{12}\text{C}$ and $^{12}\text{C}+^{197}\text{Au}$ reactions at 62 A MeV. In this work, the measured ^4He cross sections angular distributions at four selected angles are presented and compared.

DOI:10.5506/APhysPolB.45.565

PACS numbers: 87.53.-j, 87.55.D-, 25.70.Mn

* Presented at the XXXIII Mazurian Lakes Conference on Physics, Piaski, Poland, September 1–7, 2013.

† Deceased.

1. Introduction

The choice of applying heavy-ion beams in tumor therapy relies on their highly localized dose distribution at the end of the penetration depth in the tissue (the Bragg Peak) and their improved relative biological effectiveness (RBE) for treating radio-resistant tumors with respect to photons or proton radiotherapy. Among the different ion species, carbon represents the best compromise in terms of both spatial selectivity and tumor sterilization capability. Thanks to these advantages, carbon beams are currently used in some hadrontherapy facilities around the world [1].

Unfortunately, the main drawback of carbon ions treatment is related with the production of lighter fragments within the patient tissue, as far as the primary beam may undergo inelastic nuclear reactions along the radiation range. The resulting spatial dose distribution, both inside and outside the tumor region, is thus altered by secondary fragments, having longer ranges and broader angular distributions with respect to the beam. Additionally, the carbon ions RBE has to be replaced by the one associated with the arising mixed radiation field, as far as the RBE depends strongly on the linear energy transfer (LET) value, which is different for each isotope. Therefore, all these effects arising from the carbon fragmentation have to be correctly evaluated when planning a tumor treatment.

The nuclear interactions of the incident ions must be taken into account, not only in hadrontherapy, but also in understanding and addressing the effects of the galactic cosmic rays on humans in space. One of the most serious problem for space missions outside the Earth's magnetic field is the radiobiological risk for the astronauts [2]. In order to correctly evaluate such risk, the nuclear reactions of the galactic cosmic rays inside the shielding materials of the space shuttle and the astronaut bodies must be considered. The particles and energies commonly used for hadrontherapy overlap the low end of the charge and energy range of greatest interest for space radiation applications, *i.e.* $Z = 1-26$ and approximately 100–1000 MeV/nucleon. Moreover, the incident ions lose their energy passing through the patient's body so that the inelastic nuclear reactions may occur at energies much lower than the incident ones.

In planning tumor treatments and space missions, the only way to overcome the approximations of analytical calculations in the case of mixed radiation fields and complex geometries is the use of reliable Monte Carlo codes, such as Geant4 [3]. However, in order to precisely simulate the spatial dose distribution and the resulting biological effects in the human body, the physical models used in the Monte Carlo codes need to be tuned and validated by experimental fragmentation data. With the aim to measure fragmentation cross sections, some dedicated experiments have been already performed at relativistic energies [4]. Since at Fermi energies only a small amount of data

are available in literature, we decided to fill this gap measuring an extensive set of fragmentation cross sections in this energy regime. Particularly, we studied both $^{12}\text{C}+^{12}\text{C}$ and $^{12}\text{C}+^{197}\text{Au}$ reactions at 62 A MeV. In the following, we focused on ^4He production cross sections by comparing the results obtained with the ^{12}C target, already published [5], with those obtained with the ^{197}Au target.

2. Experimental setup

The experiment was performed at the Superconducting Cyclotron (CS) of the INFN — LNS in Catania. A ^{12}C beam was accelerated at 62 A MeV and sent to a $104\ \mu\text{g}/\text{cm}^2$ and a $147\ \mu\text{g}/\text{cm}^2$ thick ^{12}C and ^{197}Au target. Energy and emission angle of charged fragments ($1 \leq Z \leq 5$) produced in the interaction with the target were measured by a detection setup consisting of two Si–CsI hodoscopes [6]:

- The Hodo-Small — formed by 81 two-fold telescopes: $300\ \mu\text{m}$ silicon detectors $1 \times 1\ \text{cm}^2$ of active area followed by a $1 \times 1\ \text{cm}^2$ and 10 cm long CsI(Tl);
- The Hodo-Big — formed by 88 three-fold telescopes: $50\ \mu\text{m} + 300\ \mu\text{m}$ silicon detectors both having $3 \times 3\ \text{cm}^2$ surface followed by a 6 cm long CsI(Tl).

In the present experiment, the Hodo-Small was placed 80 cm from the target, covering the angular region between $2.2^\circ \leq \vartheta_{\text{lab}} \leq 5.5^\circ$. The Hodo-Big was placed at 60 cm from the target covering the angular region between $7.6^\circ \leq \vartheta_{\text{lab}} \leq 21.8^\circ$. Fragments detected in each telescope were identified in charge and mass by using the ΔE – E_{res} identification technique, being ΔE and E_{res} the energy loss and the residual energy measured in the Si and CsI detectors, respectively. The absolute cross sections were determined from the measured fragment yields, corrected for the acquisition system dead-time ($\sim 1\ \text{msec}$), the target thickness and the beam current ($\sim 100\ \text{nA}$) measured with a Faraday cup. The uncertainties in the cross sections result from the statistical errors in the fragment yields, the uncertainties on the target thickness, the number of incident ions and the dead-time.

3. ^4He cross sections angular distributions

In Fig. 1, the measured angular distributions of the ^4He production cross sections $d\sigma/d\Omega$ in the $^{12}\text{C}+^{12}\text{C}$ and $^{12}\text{C}+^{197}\text{Au}$ reactions at $\vartheta_{\text{lab}} = 8.2^\circ$, 14.4° , 18.0° and 21.8° are shown. As one can clearly see, both angular distributions fall exponentially, indicating that the ^4He is mostly emitted at

forward angles. Nevertheless, at large angles it seems that α particles production is still relevant, so that the associated broadening of the spatial dose distribution has to be carefully taken into account for both hadrontherapy and space radiation protection purposes.

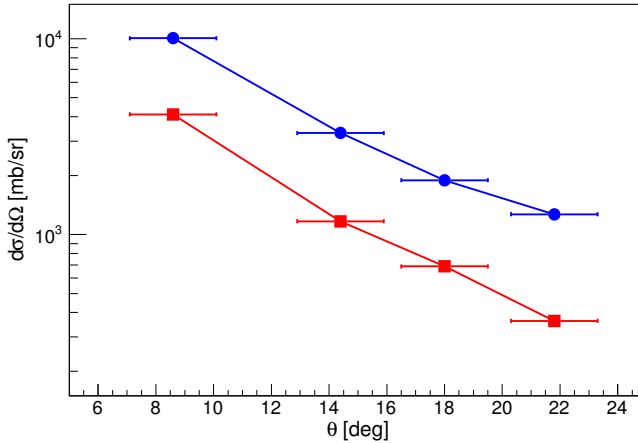


Fig. 1. Experimental cross sections angular distributions for the ^4He production in the $^{12}\text{C} + ^{12}\text{C}$ (\blacksquare) and $^{12}\text{C} + ^{197}\text{Au}$ (\bullet) reactions at $\vartheta_{\text{lab}} = 8.2^\circ, 14.4^\circ, 18.0^\circ$ and 21.8° . Error bars on the cross sections are smaller than the markers size. The exponential best-fits of the data are also shown (solid lines).

The comparison between the absolute cross section values extracted from the two data sets shows a strong target dependence, being those measured with the ^{197}Au target significantly higher than those measured with the ^{12}C target.

This target-size effect has been already observed at relativistic energies, the so-called factorization, and is considered a basic law of the projectile fragmentation reactions [7, 8]. As a consequence, the enhancement of ^4He production cross sections observed for the heavier target can be associated to the geometrical properties of the colliding system, *i.e.* to the greater target nucleus size. At Fermi energies, different dissipative reaction mechanisms can contribute, together with the fragmentation one, to the fragment production at different ϑ_{lab} [5].

In order to better investigate the role of the other dissipative reactions in the observed target dependence, a detailed analysis of the fragment energy spectra and their evolution as a function of the emission angle is in progress.

4. Conclusions

Fragmentation cross sections related to $^{12}\text{C}+^{12}\text{C}$ and $^{12}\text{C}+^{197}\text{Au}$ reactions at 62 A MeV have been measured at the LNS. A strong dependence of the cross sections on the target has been observed by comparing the two measured data sets for the α particles production. These experimental data will be used to improve the prediction capability of the nuclear reaction models implemented in the Monte Carlo codes, as requested in both carbon ion therapy and radioprotection of humans in space.

REFERENCES

- [1] D. Schardt, T. Elsasser, *Rev. Mod. Phys.* **82**, 383 (2010).
- [2] M. Durante, F.A. Cucinotta, *Rev. Mod. Phys.* **83**, 1245 (2011).
- [3] S. Agostinelli *et al.*, *Nucl. Instrum. Methods* **A506**, 250 (2003).
- [4] R. Pleskac *et al.*, *Nucl. Instrum. Methods* **A678**, 130 (2012).
- [5] M. De Napoli *et al.*, *Phys. Med. Biol.* **57**, 7651 (2012).
- [6] G. Raciti *et al.*, *Phys. Rev. Lett.* **100**, 192503 (2008).
- [7] D.L. Olson *et al.*, *Phys. Rev.* **C28**, 1602 (1983).
- [8] J.R. Cummings Olson *et al.*, *Phys. Rev.* **C42**, 2530 (1990).